

## Toward a stability analysis of inhomogeneous phases in QCD

Theo F. Motta,<sup>1,2</sup> Julian Bernhardt<sup>1</sup>, Michael Buballa,<sup>2,3</sup> and Christian S. Fischer<sup>1,4</sup>

<sup>1</sup>*Institut für Theoretische Physik, Justus-Liebig-Universität Gießen, 35392 Gießen, Germany*

<sup>2</sup>*Technische Universität Darmstadt, Fachbereich Physik, Institut für Kernphysik, Theoriezentrum, Schlossgartenstr. 2D-64289 Darmstadt, Germany*

<sup>3</sup>*Helmholtz Forschungsakademie Hessen für FAIR (HFHF), GSI Helmholtzzentrum für Schwerionenforschung, Campus Darmstadt, 64289 Darmstadt, Germany*

<sup>4</sup>*Helmholtz Forschungsakademie Hessen für FAIR (HFHF), GSI Helmholtzzentrum für Schwerionenforschung, Campus Gießen, 35392 Gießen, Germany*

 (Received 28 June 2023; accepted 18 November 2023; published 18 December 2023)

The possible occurrence of crystalline or inhomogeneous phases in the QCD phase diagram at large chemical potential has been under investigation for over thirty years. Such phases are present in *models* of QCD such as the Gross-Neveu model in  $1 + 1$  dimensions, Nambu–Jona-Lasinio (NJL) and quark meson models. Yet, no unambiguous confirmation exists from actual QCD. In this work, we propose a new approach for a stability analysis that is based on the two-particle irreducible effective action and compatible with full QCD calculations within the framework of functional methods. As a first test, we reproduce a known NJL model result within this framework. We then discuss the additional difficulties which arise in QCD due to the nonlocality of the quark self-energy and suggest a method to overcome them. As a proof of principle and as an illustration of the analysis, we consider the Wigner-Weyl solution of the quark Dyson-Schwinger equation (DSE) within a simple truncation of QCD in the chiral limit and analyze its stability against *homogeneous* chiral-symmetry breaking fluctuations. For temperatures above and below the tricritical point we find that the boundary of the instability region coincides well with the second-order phase boundary or the left spinodal, respectively, obtained from the direct solutions of the DSEs. Finally, we outline how this method can be generalized to study inhomogeneous fluctuations.

DOI: [10.1103/PhysRevD.108.114019](https://doi.org/10.1103/PhysRevD.108.114019)

### I. INTRODUCTION

At high densities and low temperatures, systems of interacting fermions may form crystalline, i.e., spatially inhomogeneous phases. Unsurprisingly, systems governed by the strong interaction are no exception. The idea of density waves in nuclear matter dates back to Overhauser in 1960 [1], followed by Migdal’s renowned works on p-wave pion condensation in the 1970s [2,3]. A first relativistic treatment of chiral-density waves (CDWs) in nuclear matter was presented in Ref. [4], while already in 1990 the idea was transferred to quark matter [5] (see Ref. [6] for a brief review on those early works). In the early 2000s, the possible existence of color superconducting (CSC) phases attracted much attention [7], and in this context both

crystalline CSC phases [8–14] as well as inhomogeneous chiral phases in coexistence with homogeneous CSC phases [15,16] have been explored. Roughly at the same time, sophisticated analyses of the  $1 + 1$  dimensional Gross-Neveu (GN) and chiral GN models in the large- $N$  limit revealed not only the existence of inhomogeneous phases in these models but also the exact shapes of the inhomogeneities [17–20]. The discovery that these lower-dimensional solutions could also be embedded into higher dimensions [21] triggered further studies in particular in the Nambu–Jona-Lasinio (NJL) and quark-meson (QM) models, which seemed to confirm that inhomogeneous phases are a rather robust feature of this kind of models (see Ref. [22] for a review).

However, while the existence of inhomogeneous phases has rigorously been proven for the  $1 + 1$  dimensional GN and chiral GN models in the large- $N$  limit, recent works within higher dimensional NJL and GN models signal the possibility that inhomogeneous phases may only appear as cutoff artefacts [23–25], also see Refs. [26,27] for early studies on cutoff effects. This casts some general doubt that models that are nonrenormalizable and, consequentially,

---

*Published by the American Physical Society under the terms of the Creative Commons Attribution 4.0 International license. Further distribution of this work must maintain attribution to the author(s) and the published article’s title, journal citation, and DOI. Funded by SCOAP<sup>3</sup>.*

cutoff dependent, could ever produce trustworthy results concerning such phases.

It is thus an interesting and open question, whether inhomogeneous phases exist in actual quantum chromodynamics (QCD). In fact, it was shown in Refs. [28,29] that, for large number of quark colors  $N_c$ , homogeneous quark matter at high density is unstable against the formation of chiral waves—a phase in which chiral symmetry is inhomogeneously broken [30]. Yet Ref. [29] also showed that this was unlikely to happen at  $N_c = 3$ , for which they are strongly disfavored against CSC phases. These analyses, however, rely on weak-coupling expansions, which are valid only at very high densities. They are therefore not applicable to the phenomenologically more interesting nonperturbative regime between about one and a few times nuclear saturation density.

On the other hand, since this regime is not accessible by lattice simulations either, the question about the existence of inhomogeneous chiral phases in QCD has to be addressed with functional methods. In Ref. [32], where three-flavor QCD was investigated within the functional renormalization group, indications of inhomogeneity in a region around the critical endpoint have been observed but the finding was not fully conclusive [33]. Within a truncation of the (renormalized) Dyson-Schwinger equations (DSE) of QCD Ref. [34] managed to find an inhomogeneous solution to the quark propagator at finite density. However, the analysis was restricted to a particular *Ansatz* for the inhomogeneity, making it extremely difficult to improve the truncation.

In this work, we therefore aim at developing a more flexible approach to study the existence of inhomogeneous phases in QCD. We propose a generalization of the stability analyses that have successfully been applied to models like NJL [24,35,36], GN [23,37] or the QM [38] model. In its new form the method is not only applicable to renormalizable theories such as QCD but also to beyond mean-field applications of NJL and QM models.

The paper is organized as follows: In order to place our work in the context of previous approaches, we briefly review in Sec. II how inhomogeneous phases are studied within models, putting particular emphasis on stability analyses in the NJL model. As we will discuss, this method cannot immediately be applied to QCD. In Sec. III we will therefore present a new framework using the 2PI effective action of QCD. We then follow with a small number of general remarks on potential generalizations to nPI effective actions. In Sec. IV, as a first test, we apply the approach again to the NJL model and show that we can reproduce the known results. Then, in Sec. V we discuss additional difficulties which arise in QCD as compared to the NJL model and propose a method how to overcome them. In Sec. VI we perform a first numerical test of this approach by applying it to study the second-order transition from the *homogeneous* chirally broken to the chirally restored phase

in the chiral limit of (a truncation of) QCD and comparing the result to that from directly solving the corresponding DSE. As we will see, this gives vital clues as to the working of the method and how to extend it to study inhomogeneous phases. We conclude this work with a short summary and an outlook toward more sophisticated calculations within QCD.

## II. MODEL STUDIES OF INHOMOGENEOUS PHASES

As mentioned above, most studies of inhomogeneous phases in strong-interaction matter have been performed within QCD inspired models. In addition simplifications have been used, since it is a nontrivial matter to study phases which break translational symmetry. Most commonly, two approaches are available. First, one might propose an *ad hoc Ansatz* for an inhomogeneous phase and simply verifies whether or not this proposed *Ansatz* phase is more stable than the homogeneous one (by comparing their free energies). Alternatively, one may perform a stability analysis of the homogeneous phase, i.e., one determines whether or not the homogeneous phase is unstable against small inhomogeneous fluctuations of *any* shape. Both NJL, GN and QM studies have been carried out within these two approaches (see, e.g., [36–41] and references therein).

As an illustration, take the standard NJL model

$$\mathcal{L}_{\text{NJL}} = \bar{\psi}(i\cancel{\partial} - m)\psi + G \sum_M (\bar{\psi} V^{(M)} \psi)^2 \quad (1)$$

where  $\psi$  denotes a quark field with two flavor degrees of freedom and bare mass  $m$ . The second term with coupling constant  $G > 0$  and vertices  $V^{(M)} \in \{\mathbf{1}, i\gamma_5 \tau_a\}$ , where  $\tau_a$ ,  $a = 1, 2, 3$ , are the Pauli matrices in isospin space, correspond to four-point interactions in the scalar-isoscalar and pseudoscalar-isovector channels. Assuming the presence of the (possibly inhomogeneous) condensates

$$\phi_M(\vec{x}) = \langle \bar{\psi}(\vec{x}) V^{(M)} \psi(\vec{x}) \rangle, \quad (2)$$

the mean-field thermodynamic potential, corresponding to the free-energy density, then takes the form

$$\Omega_{\text{MF}} = -\frac{T}{V} \text{Tr} \log \left( \frac{S^{-1}}{T} \right) + G \sum_M \frac{1}{V} \int d^3x \phi_M^2(\vec{x}), \quad (3)$$

where

$$S^{-1} = S_0^{-1} + 2G \sum_M V^{(M)} \phi_M(\vec{x}) \quad (4)$$

is the inverse dressed quark propagator and  $S_0^{-1}$  is its bare counterpart.  $T$  is the temperature, while the chemical

potential is hidden in the bare propagator. The functional trace  $\text{Tr}$  is over internal degrees of freedom as well as the Euclidean four-volume  $V_4 = [0, \frac{1}{T}] \times V$  with the spatial volume  $V$ , which will be sent to infinity.

It is important to note that the quark self-energy  $\Sigma = S^{-1} - S_0^{-1}$  is a linear combination of the condensates. This is a feature of mean-field NJL, which is absent in QCD. It allows us to view the mean-field thermodynamic potential as a functional of the condensates,  $\Omega_{\text{MF}} = \Omega_{\text{MF}}[\phi_M]$ . Yet, in order to determine the ground state of the system, we have to minimize  $\Omega_{\text{MF}}$  with respect to the condensates, which is a nontrivial task as their spatial shapes are unknown [42].

In this context, basically two strategies have been employed in the literature. The first one consists in making a direct *Ansatz* for the condensates with a finite number of parameters and then minimizing the free energy with respect to these parameters. Probably the most popular example is the chiral density wave (CDW) [4,5,43],

$$\phi_S(\vec{x}) = -\frac{\Delta}{2G} \cos(\vec{q} \cdot \vec{x}), \quad \phi_{P,3}(\vec{x}) = -\frac{\Delta}{2G} \sin(\vec{q} \cdot \vec{x}), \quad (5)$$

with parameters  $\Delta$ , related to the amplitude, and a wave vector  $\vec{q}$ . This *Ansatz* corresponds to a rotation in the plane of scalar ( $V^{(S)} = \mathbf{1}$ ) and pseudoscalar ( $V^{(P,3)} = i\gamma_5\tau_3$ ) condensates as one goes along the direction of the wave vector  $\vec{q}$ . A more sophisticated *Ansatz* is the real-kink-crystal (RKC) [21], where the scalar condensate takes the form of a Jacobi elliptic function,  $\phi_S(x) = \Delta\sqrt{\nu}/2G\text{sn}(\Delta x/\nu)$ , with elliptic modulus  $\nu$ . Other examples studied are one- and two-dimensional sinusoidal shapes in the scalar sector [44]. All of these shapes were typically found to be favored over the homogeneous phase in a certain region of the phase diagram, with the RCS *Ansatz* being the most favored one studied so far [22].

The alternative approach is performing a stability analysis of the homogeneous ground state, i.e., the homogeneous state with the lowest free energy. In contrast to the direct *Ansatz* approach it has the advantage of being “modulation shape agnostic.” This may be a real benefit, since in practice we usually do not know the exact shape the inhomogeneous modulation takes [45]. On the downside, since the analysis relies on continuity, discontinuous first-order transitions to inhomogeneous phases may not show up in a stability analysis.

Specifically, one expands the free energy in Eq. (3) around the homogeneous state. The condensates are then expressed as

$$\phi_M(\vec{x}) = \bar{\phi}_M + \delta\phi_M(\vec{x}), \quad (6)$$

where in this paper we indicate quantities in the homogeneous ground state with a bar. So  $\bar{\phi}_M$  denotes the

condensates in the homogeneous ground state while the  $\delta\phi_M(x)$  are small, possibly inhomogeneous, perturbations around them. We then expand

$$\Omega_{\text{MF}} = \sum_{n=0}^{\infty} \Omega^{(n)}, \quad \Omega^{(n)} \propto \mathcal{O}(\delta\phi^n) \quad (7)$$

where each contribution  $\Omega^{(n)}$  is of the  $n$ th power in the fluctuations. Obviously, the zeroth order is the homogeneous case

$$\Omega_{\text{NJL}}^{(0)} = -\frac{T}{V} \text{Tr} \log\left(\frac{\bar{S}^{-1}}{T}\right) + G \sum_M \bar{\phi}_M^2, \quad (8)$$

where  $\bar{S}^{-1}$  is the inverse quark propagator Eq. (4) evaluated for  $\phi_M = \bar{\phi}_M$ .

The first-order term  $\Omega^{(1)}$  vanishes by the quark gap equation [35], and therefore the leading-order fluctuation contribution is the second-order term, which can be written as

$$\Omega^{(2)} = \frac{2G^2}{V} \sum_M \int_{\vec{q}} |\delta\phi_M(\vec{q})|^2 D_M^{-1}(q) \quad (9)$$

where the  $\delta\phi_M(\vec{q})$  is the Fourier transform [46] of  $\delta\phi_M(\vec{x})$  and

$$D_M^{-1}(q) = \frac{1}{2G} + \sum_k \text{tr}[V^{(M)}\bar{S}(k)V^{(M)}\bar{S}(k+q)] \quad (10)$$

can be interpreted as inverse (unrenormalized) meson propagators within the NJL model. Here “tr” denotes a trace over internal (color, flavor, and Dirac) degrees of freedom, and we introduced the shorthand notations

$$\int_{\vec{k}} \equiv \int \frac{d^3k}{(2\pi)^3}, \quad \sum_k \equiv T \sum_{\omega_n} \int \frac{d^3k}{(2\pi)^3} \quad (11)$$

where momenta are generically given by  $k = (\vec{k}, k_4 = \omega_k)$ , with fermionic Matsubara frequencies  $\omega_k = (2n+1)\pi T$ .

Note that, since we only allow for spatial inhomogeneities but still assume that the fluctuations are time-independent,  $\delta\phi_M(\vec{q})$  only depends on the three-momentum  $\vec{q}$ , which is integrated over in Eq. (9). The argument  $q$  of  $D_M^{-1}$  is then the corresponding four-momentum vector with zero energy. Moreover, since we are expanding about a homogeneous and therefore isotropic state,  $D_M^{-1}$  effectively only depends on  $|\vec{q}|$ .

An important feature of Eq. (9) is that the integrand depends on the squared modulus of  $\delta\phi_M(\vec{q})$ , so the only way this can ever be negative, and thus, lower the free

energy, is by having the inverse meson propagators  $D_M^{-1}(q)$  be negative for certain momenta. This is actually a sufficient criterion for instability because, even if  $D_M^{-1}(q)$  is negative only in a small momentum regime, any fluctuation which has support only in that regime will lower the free energy. The phase boundary can then be identified as a line in the  $T - \mu$  plane where one of the  $D_M^{-1}$  touches zero at a single value of  $|\vec{q}|$ .

As obvious from Eq. (10), in the limit of vanishing interactions the positive constant  $1/2G$  dominates and no instability occurs. On the other hand, the integral is negative, as we will discuss below. Therefore, it is easy to see how, if the interaction coupling  $G$  is large enough, the second term wins over the first term and the inverse propagator becomes negative.

Note that the stability analysis remains blind as to the nature of the instability. Thus, ideally, the two methods can be combined. Once the stability analysis reveals the homogeneous state to be unstable in general one can use the *Ansatz* method to search for specifically favored inhomogeneous states.

Naturally, the trade-off for such a generality is the fact that stability analyses can only identify second-order phase transitions. This makes it a natural companion (rather than a competitor) of the *Ansatz* approach. In model studies where both methodologies have been applied, the boundary between the restored phase and the inhomogeneous phase is usually second-order and both methods agree on the same phase boundary.

### A. Beyond models of QCD

Within full QCD—or with any approximated technique that can be systematically improved toward full QCD—the same two choices remain, direct *Ansatz* or stability analysis. As already noted above, in Ref. [34] a chiral density wavelike *Ansatz* was tested for QCD within a DSE framework and a region of the phase diagram was found which allows for self-consistent solutions of the inhomogeneous DSEs with a CDW-like shape.

As for a stability analysis, no such work exists as of yet. Besides QCD being far more complicated to work numerically, this is mostly due to the fact that the current framework described above is not suited for QCD. One cannot write the thermodynamic potential  $\Omega$  as a functional of the condensates as for NJL and other models. This is because, in QCD, the self-energy or the inverse propagators are not simple linear combinations of the condensates. In fact, the same problem would appear beyond mean-field in NJL or QM models [47]. Therefore, the main goal of this paper is to show an alternative method to perform a stability analysis that both reproduces the classic NJL results and is applicable to QCD, beyond mean-field models, and, in fact, any field theory.

## III. 2PI EFFECTIVE ACTION STABILITY ANALYSIS

In order to formulate the framework for a general stability analysis, it is first useful to recall some basic facts. In a classical field theory, the system tends toward minima of the classical action  $S_{\text{cl}}$ . The equations of motion of the theory are given by extrema conditions  $\delta S_{\text{cl}}/\delta\phi = 0$  of the classical action with respect to the fields. In a quantum field theory, the effective action  $\Gamma$  plays the same role and the corresponding quantum equations of motion, the Dyson-Schwinger equations, are found by exactly the same logic. Also, the effective action is a proxy for the pressure and other thermodynamic quantities of the theory. The thermodynamic potential,  $\Omega$ , at finite temperature  $T$  and finite chemical potential  $\mu$  is found by subtracting the vacuum term [54]

$$\Omega(T, \mu) = -\frac{T}{V}(\Gamma(T, \mu) - \Gamma(0, 0)) = -\frac{T}{V}P(T, \mu). \quad (12)$$

Furthermore, one can write the effective action of a theory as a functional of the n-point functions of the fields, the inverse propagators and vertices (see e.g., the C and Refs. [55,56]).

Starting from a 2-particle-irreducible (2PI) effective action [57] such as

$$\Gamma = \text{Tr} \log[S^{-1}] - \text{Tr}[\mathbf{1} - S_0^{-1}S] + \Phi_{2\text{PI}}[S], \quad (13)$$

where,  $S$  is the full propagator,  $S_0$  the bare one, and  $\Phi_{2\text{PI}}[S]$  is the sum of all 2PI diagrams, we find the Dyson-Schwinger equations by

$$\frac{\delta\Gamma}{\delta S} = 0 \Rightarrow -S^{-1} + S_0^{-1} + \frac{\delta\Phi_{2\text{PI}}}{\delta S} = 0 \Rightarrow S^{-1} = S_0^{-1} + \Sigma, \quad (14)$$

where we identified the derivative of  $\Phi_{2\text{PI}}$  with the self-energy  $\Sigma$ . Solutions to the equation above will reveal every stable, unstable or metastable equilibrium configuration of the system. Let  $\bar{S}$  be an equilibrium solution, namely the homogeneous configuration. We may analyze if it is stable or not by taking

$$S = \bar{S} + \delta S.$$

where  $\delta S$  is a small inhomogeneous propagator (what sufficiently “small” means is described in a later section). We can then take a functional Taylor expansion around the  $\delta S = 0$  point

$$\Gamma[S] = \Gamma[\bar{S}] + \text{Tr} \left[ \frac{\delta\Gamma}{\delta S_{xy}} \delta S_{yx} \right] + \frac{1}{2!} \text{Tr} \left[ \frac{\delta^2\Gamma}{\delta S_{xy} \delta S_{zs}} \delta S_{yx} \delta S_{sz} \right] + \dots \quad (15)$$



where we again use the bar notation  $\bar{O}$  to denote  $O$  evaluated at the homogeneous solution. The indices on the various  $\delta S$  will from now on be omitted and taken to be implicitly understood (see Appendix B). We then have

$$\begin{aligned}\Gamma^{(0)} &= -\text{Tr} \log[\bar{S}] - \text{Tr}[\mathbf{1} - S_0^{-1} \bar{S}] + \Phi_{2\text{PI}}[\bar{S}] \\ \Gamma^{(1)} &= \text{Tr} \left[ \left( -\bar{S}^{-1} + S_0^{-1} + \frac{\overline{\delta\Phi_{2\text{PI}}}}{\delta S} \right) \delta S \right] \\ \Gamma^{(2)} &= \frac{1}{2} \text{Tr}[(\bar{S}^{-1} \delta S)^2] + \frac{1}{2} \text{Tr} \left[ \frac{\overline{\delta^2 \Phi_{2\text{PI}}}}{\delta S \delta S} \delta S \delta S \right]\end{aligned}\quad (16)$$

where  $\Gamma^{(0)}$  is the homogeneous effective action,  $\Gamma^{(1)}$  vanishes at the stationary point [58], and the thermodynamic potential

$$\Omega^{(2)}(T, \mu) = -\frac{T}{V} (\Gamma^{(2)}(T, \mu)) \quad (17)$$

arising from  $\Gamma^{(2)}$  is our starting point for the stability analysis.

### A. Some remarks on the $n\text{PI}$ case

The approach described above is not solely applicable to 2PI effective actions. A brief look at the more general case may be enlightening. Take a 1PI effective action, which is characterized by the Legendre transform of the connected generating functional  $W$  in the presence of a one-point source  $J$ ,

$$\Gamma[\phi] = W[J] - \phi_i J_i, \quad (18)$$

where here we use the standard simplified notation of two repeated indices implying sum and integration of all discrete indices and continuum variables respectively. As per usual, the root of

$$\frac{\delta \Gamma}{\delta \phi_i} = -J_i, \quad (19)$$

defines the physical point, and our one-point function—most generally, in the presence of sources—is

$$\frac{\delta W}{\delta J_i} = \phi_i. \quad (20)$$

The second derivatives yield the following relations

$$\frac{\delta^2 \Gamma}{\delta \phi_i \delta \phi_j} = -\frac{\delta J_i}{\delta \phi_i}, \quad \frac{\delta^2 W}{\delta J_i \delta J_j} = \frac{\delta \phi_i}{\delta J_j}. \quad (21)$$

Assuming, as per usual, invertibility of  $\phi[J]$ , we obtain

$$\frac{\delta^2 \Gamma}{\delta \phi_i \delta \phi_j} = -\left( \frac{\delta^2 W}{\delta J_j \delta J_i} \right)^{-1}. \quad (22)$$

It is an elementary result in quantum field theory that  $n$  derivatives of the generating functional  $W$  with respect to the one-point sources  $J$  yield the connected  $n$ -point functions (see Appendix C). Therefore, Eq. (22) shows that the second derivative of the 1PI effective action with respect to the 1-point function is (minus) the inverse 2-point function [59] in the presence of sources.

Note, however, that the NJL result in Eq. (9) is based on a 1PI approach. This comes from the fact that the model is written as a field theory of the mean-field condensates (the  $\Omega_{\text{MF}}^{\text{NJL}}[\phi]$  defined above). The question is, can this approach be generalized? Indeed, take a 2PI effective action, i.e., a functional of two functions whose stationary point defines *self-consistently* the one-point and two-point functions

$$\Gamma[\phi, S] = W[J, R] - \phi_i J_i - S_{ij} R_{ij}. \quad (23)$$

The same game can be played and we obtain

$$\frac{\delta^2 \Gamma}{\delta \phi_i \delta \phi_j} = -\frac{\delta J_i}{\delta \phi_i}, \quad \frac{\delta^2 W}{\delta J_i \delta J_j} = \frac{\delta \phi_i}{\delta J_j}, \quad \frac{\delta^2 \Gamma}{\delta \phi_i \delta \phi_j} = -\left( \frac{\delta^2 W}{\delta J_j \delta J_i} \right)^{-1}, \quad (24)$$

$$\begin{aligned}\frac{\delta^2 \Gamma}{\delta S_{ij} \delta S_{kl}} &= -\frac{\delta R_{ij}}{\delta S_{kl}}, & \frac{\delta^2 W}{\delta R_{ij} \delta R_{kl}} &= \frac{\delta S_{ij}}{\delta R_{kl}}, \\ \frac{\delta^2 \Gamma}{\delta S_{ij} \delta S_{kl}} &= -\left( \frac{\delta^2 W}{\delta R_{kl} \delta R_{ij}} \right)^{-1}\end{aligned}\quad (25)$$

The second derivative of  $W$  with respect to the two-point source  $R$  is the *inverse* four-point function. If we now revisit Eq. (15) we see that, at the physical point, it is trivial that  $\Gamma^{(1)}$  always vanishes and  $\Gamma^{(2)}$  is given by (minus) the inverse 2-point function. Therefore, if we assume both the one- and two-point functions can be inhomogeneous, our instability condition will be, analogously to Eq. (15), given by

$$\Gamma^{(2)} = \frac{1}{2!} \text{Tr} \left[ \frac{\overline{\delta^2 \Gamma}}{\delta \phi_x \delta \phi_y} \delta \phi_x \delta \phi_y \right] + \frac{1}{2!} \text{Tr} \left[ \frac{\overline{\delta^2 \Gamma}}{\delta S_{xy} \delta S_{zs}} \delta S_{yx} \delta S_{sz} \right] \quad (26)$$

and thus, negativity of the connected two-point function or the connected four-point function will signal an instability. In QCD we do not have an analogous to the one-point function  $\phi$ . Therefore, an instability will be signalled by negativity of the four-point functions of the theory.

It is trivial to see how this can be generalized to any  $m$ -loop  $n\text{PI}$  effective action and the instability condition will always be given by negativity of the inverse  $2n$ -point functions. More explicitly, take an  $n\text{PI}$  effective action

$$\Gamma[\phi, S_2, S_3, S_4, \dots, S_n],$$

which at the stationary point gives, self-consistently, the fully-dressed  $n$ -point functions of the theory. Negativity of the second derivative of  $\Gamma$  with respect to any  $\phi, S_2, S_3, S_4, \dots, S_n$  at the stationary point—or, in other terms, negativity of any of the inverse two-particle, four-particle, ...,  $2n$ -particle connected Green's functions—is the instability condition.

#### IV. APPLICATION TO THE NJL MODEL

As a first test, we apply the method developed in Sec. III to the NJL model, Eq. (1). In Hartree approximation, which was also the basis of Eqs. (9) and (10), we have the 2PI functional

$$\Phi_{2\text{PI}} = G \int_{x,y} \delta(x-y) \sum_M \text{tr}[V^{(M)} S(x,x)] \times \text{tr}[V^{(M)} S(y,y)] \quad (27)$$

with the vertices  $V^{(M)}$  defined below Eq. (1) and the integrals are taken over the Euclidean four-volume. As before the, lower case “tr” notation means a trace over internal degrees of freedom. From Eq. (14) we then obtain the quark self-energy

$$\begin{aligned} \Sigma(x,y) &= \frac{\delta\Phi_{2\text{PI}}}{\delta S(y,x)} \\ &= 2G\delta(x-y) \sum_M \text{tr}[V^{(M)} S(x,x)] V^{(M)} \\ &\equiv \Sigma(x)\delta(x-y), \end{aligned} \quad (28)$$

making explicit that the self-energy is local, i.e., depends only on a single space-time coordinate. Of course, this is an expected consequence of the local four-point interaction together with the Hartree approximation, but it will become important later on.

In homogeneous (= translational invariant) matter the propagator depends only on space-time differences,  $\bar{S} = \bar{S}(x-y)$ , so that the self-energy becomes constant:

$$\bar{\Sigma}(x) = 2G \sum_M \text{tr}[V^{(M)} \bar{S}(0)] V^{(M)} = \text{const}. \quad (29)$$

In the following, we will refer to this equation as the homogeneous gap equation.

As outlined in the previous section, we now consider small, possibly inhomogeneous, fluctuations  $\delta S(x,y)$  of the propagator around the homogeneous solution  $\bar{S}$ , and expand the effective action in powers of  $\delta S$ . At first order we obtain

$$\begin{aligned} \Gamma^{(1)} &= - \int_{x,y} \text{tr}[\bar{\Sigma}(x,y) \delta S(x,y)] \\ &\quad + 2G \sum_M \int_x \text{tr}[V^{(M)} \bar{S}(0)] \text{tr}[V^{(M)} \delta S(x,x)], \end{aligned} \quad (30)$$

where the first term on the right-hand side originates from the two functional traces in Eq. (13) and the last term is due to  $\Phi_{2\text{PI}}$ . Using the locality of the self-energy together with the homogeneous gap equation, we immediately see that  $\Gamma^{(1)} = 0$ , confirming our general expectation.

At second order we have

$$\begin{aligned} \Gamma^{(2)} &= \frac{1}{2} \int_{w,x,y,z} \text{tr}[\bar{S}^{-1}(w,x) \delta S(x,y) \bar{S}^{-1}(y,z) \delta S(z,w)] \\ &\quad + G \sum_M \int_x (\text{tr}[V^{(M)} \delta S(x,x)])^2, \end{aligned} \quad (31)$$

where we explicitly wrote the functional trace in coordinate space. Turning to momentum space this becomes

$$\begin{aligned} \Gamma^{(2)} &= \frac{1}{2} \int_{p,q} \text{tr}[\bar{S}^{-1}(p+q) \delta S(p+q, p) \bar{S}^{-1}(p) \delta S(p, p+q)] \\ &\quad + G \sum_M \int_q \left( \int_p \text{tr}[V^{(M)} \delta S(p+q, p)] \right) \\ &\quad \times \left( \int_k \text{tr}[V^{(M)} \delta S(k, k+q)] \right). \end{aligned} \quad (32)$$

As discussed, a positive  $\Gamma^{(2)}$ , corresponding to a negative contribution to the thermodynamic potential, signals an instability of the homogeneous solution. However, if we compare the above expression with Eq. (9), we see that in the latter the moduli squared of the fluctuations appear as isolated factors, so that the question about the stability of the homogeneous state could be decided solely on the sign of their coefficients  $D_M^{-1}$ . In Eq. (32), on the other hand, isolating the fluctuations from the rest is inhibited by the different momentum arguments. As a consequence, a modulation-shape agnostic stability analysis is not immediately possible on the basis of this equation.

However, we have not yet exploited the fact that the quark self-energy and, hence, its fluctuations  $\delta\Sigma$  are local. To this end it is more appropriate to expand the effective action in powers of  $\delta\Sigma$ , corresponding to fluctuations of the inverse propagator, rather than in fluctuations of the propagator itself. This can be achieved by using the Dyson series,

$$S^{-1} = \bar{S}^{-1} + \delta\Sigma \Leftrightarrow S = \bar{S} - \bar{S} \delta\Sigma S = \bar{S} - \bar{S} \delta\Sigma \bar{S} + \bar{S} \delta\Sigma \bar{S} \delta\Sigma \bar{S} - \dots = \bar{S} + \delta S, \quad (33)$$

and inserting the resulting  $\delta S$  into the above expressions up to the desired order in  $\delta\Sigma$ . Since  $\Gamma^{(1)}$  vanishes to all orders by the gap equation, we immediately see that in a  $\delta\Sigma$  expansion of the effective action the first-order term vanishes as well. Moreover, the order  $(\delta\Sigma)^2$  contributions can only arise from inserting the order  $\delta\Sigma$  propagator fluctuations  $\delta S^{(1)} = -\bar{S}\delta\Sigma\bar{S}$  into  $\Gamma^{(2)}$ . In momentum space,

as a consequence of the locality,  $\delta\Sigma$  depends only on a single momentum variable, and  $\delta S^{(1)}$  is given by

$$\delta S^{(1)}(k_1, k_2) = -\bar{S}(k_1)\delta\Sigma(k_1 - k_2)\bar{S}(k_2). \quad (34)$$

Inserting this into Eq. (32) we find

$$\tilde{\Gamma}^{(2)} = \frac{1}{2} \sum_{p,q} \text{tr}[\delta\Sigma(q)\bar{S}(p)\delta\Sigma(-q)\bar{S}(p+q)] + G \sum_M \sum_q \left( \sum_p \text{tr}[V^{(M)}\bar{S}(p+q)\delta\Sigma(q)\bar{S}(p)] \right) \left( \sum_k \text{tr}[V^{(M)}\bar{S}(k)\delta\Sigma(-q)\bar{S}(k+q)] \right), \quad (35)$$

where the tilde in  $\tilde{\Gamma}^{(2)}$  was introduced to indicate that we have now performed an expansion in  $\delta\Sigma$  rather than in  $\delta S$ .

In order to proceed we decompose the fluctuations into scalar and pseudoscalar parts,

$$\delta\Sigma(q) = \sum_M \delta\Sigma_M(q)V^{(M)}, \quad (36)$$

and pull the functions  $\delta\Sigma_M$  out of the traces. The latter vanish for unequal vertex factors  $V^{(M)} \neq V^{(M')}$ , so we are left with a single sum over  $M$  for both terms. Moreover, for local fluctuations  $\delta\Sigma_M$  are real functions in coordinate space. In momentum space they therefore satisfy the relation  $\delta\Sigma_M(-q) = \delta\Sigma_M^*(q)$  and, hence, their product is given by  $|\delta\Sigma_M(q)|^2$ . Combining all terms  $\tilde{\Gamma}^{(2)}$  can then be written as

$$\tilde{\Gamma}^{(2)} = G \sum_M \sum_q |\delta\Sigma_M(q)|^2 \sum_p \text{tr}[V^{(M)}\bar{S}(p)V^{(M)}\bar{S}(p+q)] \underbrace{\left( \frac{1}{2G} + \sum_k \text{tr}[V^{(M)}\bar{S}(k)V^{(M)}\bar{S}(k+q)] \right)}_{D_M^{-1}(q)}, \quad (37)$$

where we identified the inverse meson propagators from Eq. (10).

Again, since we assume the self-energy fluctuations to be time independent, their Fourier modes are restricted to vanishing energy,  $\delta\Sigma(q) = \frac{1}{T} \delta_{q_4,0} \delta\Sigma(\vec{q})$  see Appendix A. From Eq. (17) we then obtain for the second-order contribution of the thermodynamic potential

$$\tilde{\Omega}^{(2)} = -\frac{T}{V} \tilde{\Gamma}^{(2)} = -\frac{G}{V} \sum_M \int_{\vec{q}} |\delta\Sigma_M(\vec{q})|^2 D_M^{-1}(q) \ell_M(q), \quad (38)$$

with the loop integral

$$\ell_M(q) = \sum_p \text{tr}[V^{(M)}\bar{S}(p)V^{(M)}\bar{S}(p+q)]. \quad (39)$$

Recall that an instability of the homogeneous ground state against small fluctuations corresponds to a negative  $\Omega^{(2)}$ . However, if we compare Eq. (38) with the literature NJL result Eq. (9) an essential difference seems to be the

additional factor  $-\ell_M(q)$  in the integrand of the former. In order to get a deeper understanding of the role of this factor it is instructive to consider the limit of vanishing interactions, i.e., a free fermi gas. For this case  $\tilde{\Omega}^{(2)}$  becomes

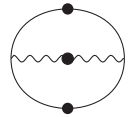
$$\tilde{\Omega}_{\text{ffg}}^{(2)} = \lim_{G \rightarrow 0} \tilde{\Omega}^{(2)} = -\frac{1}{2V} \sum_M \int_{\vec{q}} |\delta\Sigma_M(\vec{q})|^2 \ell_M(q), \quad (40)$$

showing that the stability of the free fermi gas is determined by  $\ell_M(q)$ . More precisely, since we expect the free fermi gas to be stable against inhomogeneous fluctuations, we can conclude that  $\ell_M(q)$  is always negative for  $q = (\vec{q}, q_4 = 0)$ . This physical argument is backed up by numerical calculations.

Returning to Eq. (38), the negativity of  $\ell_M(q)$  means that in the interacting case the (in)stability of the homogeneous ground state is entirely determined by the sign of the inverse meson propagators. Exactly as in Eq. (9)  $D_M^{-1}(q) < 0$  in some momentum regime indicates an instability, while the absence of such negative regions means that the homogeneous ground state is stable against

small inhomogeneous fluctuations. In this context it is interesting to note that  $D_M^{-1} = \frac{1}{2G} + \mathcal{L}_M$ . Thus, the negativity of  $\mathcal{L}_M$  which guarantees the stability of the non-interacting Fermi gas, at the same time opens the possibility for an instability in the interacting system.

So, in summary, we managed to recover the standard result, Eq. (9), within the 2PI approach. To this end, however, it was crucial to exploit the locality of the quark self-energy, which enabled us to isolate a factor  $|\delta\Sigma_M(\vec{q})|^2$  and in turn allowed for a modulation-shape agnostic stability analysis. Without utilizing the locality this was not possible, as can be seen from Eq. (32) where the different momentum arguments of the propagator fluctuations inhibit that they can be pulled out of the innermost integrals and be combined to an absolute value squared. As we will see in the next section, we will encounter the same difficulty in QCD where the gluon-mediated interaction leads to genuine nonlocal quark self-energies.

$$\Phi_{2\text{PI}}[S] = \frac{1}{2} \left( \text{diagram} \right) = \frac{1}{2} \text{Tr} \left[ \gamma_\mu t^a S(k_1, k_2) \gamma_\nu t^b S(k_2 - q, k_1 - q) D_{\mu\nu}^{ab}(q) \right] \quad (41)$$


where  $D_{\mu\nu}^{ab}$  is the gluon propagator. From Eq. (16) we get

$$\text{Tr} \left[ \frac{\delta^2 \Phi_{2\text{PI}}}{\delta S \delta S} \delta S \delta S \right] = \text{Tr} \left[ \gamma_\mu t^a \delta S(k_1, k_2) \gamma_\nu t^b \delta S(k_2 - q, k_1 - q) D_{\mu\nu}^{ab}(q) \right], \quad (42)$$

in which case the  $\delta S(k_1, k_2)$  and  $\delta S(k_2 - q, k_1 - q)$  terms *cannot* be simply factored out into a  $|\delta S|^2$ -type multiplicative factor. Thus the specific form of these terms do play a role. At some point or another in the analysis, we will have to specify what  $\delta S$  is. This brings about a few complications which need to be incorporated into the analysis, as will be discussed in the following.

Conceptually, the analysis described above is very simple. It can be framed in the following way. First, we find stationary points of the effective action (denoted by the bar notation). Then we perform the Taylor expansion which, at the end of the day, results in calculating a second derivative

$$\frac{1}{2!} \text{Tr} \left[ \frac{\delta^2 \Gamma}{\delta S_{xy} \delta S_{zs}} \delta S_{yx} \delta S_{sz} \right]. \quad (43)$$

If it shows positive/zero/negative curvature, it will indicate the stationary point is a maximum/saddle/minimum. This is a *directional derivative* in the infinite-dimensional functional space of which the propagator is an element. The natural analog with  $\mathbb{R}^N$  case is

## V. GENERAL CONSIDERATIONS FOR QCD APPLICATIONS OF THE STABILITY ANALYSIS

The application of the method described above is far more intricate for QCD than for the NJL-model and a brief discussion of such difficulties is enlightening. Recall, that our general starting point for the stability analysis is the expression Eq. (17) for the second order expansion of the thermodynamic potential. In the mean field NJL model the corresponding expressions Eq. (9) and Eq. (38) both feature the property that the inhomogeneous contribution be factorized into a “mod-squared” term such as  $|\delta\Sigma(q)|^2$  in Eq. (38) or  $|\delta\phi_M(q)|^2$  in Eq. (9). This renders a stability analysis particularly simple, since no assumptions on the specific form of the instability have to be made.

However, in QCD, even with the drastic approximation of bare quark-gluon vertices, due to the nonlocal interaction term, it will not be like this. Take the following 2PI effective potential [60]

$$\text{first : } \vec{u} \cdot \frac{\partial f(\vec{x})}{\partial \vec{x}}, \quad \text{second : } \vec{u} \cdot \frac{\partial}{\partial \vec{x}} \left( \vec{u} \cdot \frac{\partial f(\vec{x})}{\partial \vec{x}} \right),$$

i.e., the derivative of  $f$  in the  $\vec{u}$  direction, corresponds to

$$\begin{aligned} \text{first : } & \text{Tr} \left[ \frac{\delta F[\phi]}{\delta \phi(x)} \lambda(x) \right], \\ \text{second : } & \text{Tr} \left[ \frac{\delta^2 F[\phi]}{\delta \phi(x) \delta \phi(y)} \lambda(y) \lambda(x) \right], \end{aligned}$$

the derivative of  $F$  in the direction of some test-function  $\lambda(x)$ . This is sometimes denoted in the literature as  $\mathcal{D}_{\lambda(x)} F[\phi(x)]$ . What we are calculating, then, is the directional derivative of the effective action in the direction of  $\delta S = S - \bar{S}$ . In order to make this a well-defined process the test-function needs to satisfy at least the following properties:

- (i) It is a function  $\delta S: \mathbb{R}^n \rightarrow \mathbb{C}$  which must go to zero at infinity.
- (ii) It must be a “small” contribution to the propagator. This is rather subtle, however, it is sufficient to conceive of a sequence  $\delta S_\lambda$  such that  $\lim_{\lambda \rightarrow 0} \delta S_\lambda = 0$  uniformly. A “small”  $\delta S$  is then taken to be understood as a large  $\lambda$  case of  $\delta S_\lambda$ . If  $\delta S(k)_\lambda = \lambda f(k)$ , where  $f(k)$  is limited, this is sufficient. Moreover, the  $\lambda$  factors out of  $\Gamma^{(2)}$  and one can ignore it.



(iii) It must follow the propagator's adjoint relation

$$\delta S(\omega_1, \vec{k}_1, \omega_2, \vec{k}_2)^\dagger = \gamma_4 \delta S(-\omega_2, \vec{k}_2, -\omega_1, \vec{k}_1) \gamma_4, \quad (44)$$

without which the pressure can turn out complex. Taking this derivative in the direction of a test-function which does not follow these properties will lead to incorrect results. Most importantly, though, the imaginary part of the test-function must be constrained. This is because  $\Omega^{(2)}[\delta S]$  is not limited from below and every stationary point is a saddle point with respect to the imaginary part of the propagator. This is easily verified, since  $\Omega^{(2)}$  is quadratic in the  $\delta S$  function. Let  $\delta S_1$  be a real function which follows the properties listed above and such that  $\Omega^{(2)}[\delta S_1] > 0$ . Take  $\delta S_2 = i\alpha\delta S_1$ . Naturally  $\Omega^{(2)}[\delta S_2] = -\alpha^2\Omega^{(2)}[\delta S_1]$  so, the larger  $\alpha$ , the smaller the free energy. Meaning that the free energy is unlimited from below with respect to the imaginary part of  $\delta S$ . We chose then to constrain the imaginary part of the test-function by the following condition:

$$\text{Tr} \left[ \frac{\delta \Omega^{(2)}}{\delta(\delta S)} \text{Im}(\delta S) \right] = 0. \quad (45)$$

The condition in Eq. (45) fundamentally maximizes  $\Omega^{(2)}$  with respect to the imaginary part of  $\delta S$  and thus, effectively protects the analysis against false instabilities that could appear due to an inadequate  $\delta S$ . Here thereafter, Eq. (45) will be understood as an integral part of the analysis.

## VI. CHIRAL PHASE TRANSITION TEST

The approach described in Sec. III and V is not *only* valid for inhomogeneous phases. Whatever the nature of the phase transition may be, it can be tested via stability analysis as long as the energetically unfavorable phase sits either on a maximum or a saddle point of the thermodynamic potential. This is the case, for instance, for the chirally symmetric phase of massless QCD at the chiral second order phase boundary to the *homogeneous* broken phase. In this section we therefore want to test the method outlined above by applying it to study that phase transition.

In the chiral limit with vanishing explicit quark masses, QCD has a chiral-symmetric solution for all temperatures and densities, i.e., a massless propagator of the form

$$S^{-1}(k) = i\vec{k}A(k) + i(k_4 + i\mu)\gamma_4 C(k), \quad (46)$$

together with a broken, massive, solution of the form

$$S^{-1}(k) = i\vec{k}A(k) + B(k) + i(k_4 + i\mu)\gamma_4 C(k), \quad (47)$$

where A, B, and C are so-called dressing functions which emerge as a self-consistent solutions of the quark Dyson-Schwinger equation. In the high temperature/chemical potential phase, this solution is a minimum of the thermodynamic potential, whereas in the hadronic low temperature/chemical potential phase it is at a maximum and therefore unstable. We can analyse the (in)stability of such a solution by the method above, assuming the propagator is of the form

$$\begin{aligned} S(k) &= \frac{-i\vec{k}A(k) + \delta m(k) - i(k_4 + i\mu)\gamma_4 C(k)}{\vec{k}^2 A(k)^2 + (k_4 + i\mu)^2 C(k)^2} \\ &= \underbrace{\frac{-i\vec{k}A(k) - i(k_4 + i\mu)\gamma_4 C(k)}{\vec{k}^2 A(k)^2 + (k_4 + i\mu)^2 C(k)^2}}_{\bar{s} \text{ chiral}} \\ &\quad + \underbrace{\frac{\delta m(k)}{\vec{k}^2 A(k)^2 + (k_4 + i\mu)^2 C(k)^2}}_{\delta S \text{ breaks chiral symmetry}} \end{aligned} \quad (48)$$

that is, a chiral propagator plus a *small* massive term which breaks chiral symmetry ( $\delta m(k)$  is effectively a small “B” function). Using this form we may calculate  $\Gamma^{(2)}$  explicitly. Note that in this case (chiral instability) we explicitly know the form of the instability [Eq. (48)] and what is left is to explore different forms of the mass function  $\delta m(k)$  in our test-function.

### A. Truncation

In order to be able to carry out the explicit numerical calculations, we need to specify the truncation of QCD. The exact DSE for the quark propagator is shown diagrammatically in Fig. 1.

In explicit form the DSE equation in homogeneous matter reads:

$$\begin{aligned} [S(k)]^{-1} &= Z_2 [S_0(k)]^{-1} \\ &\quad + C_F Z_{1F} g^2 \int_q \gamma_\mu S(q) \Gamma_\nu(k, q; l) D_{\mu\nu}(l), \end{aligned} \quad (49)$$

where the momentum routing is  $l = (k - q)$ ,  $C_F = \frac{N_c^2 - 1}{2N_c}$  is the Casimir operator with  $N_c = 3$ , and all Zs are

FIG. 1. The DSE for the quark propagator. Note that two factors of  $i$  stemming from the Euclidean quark-gluon vertices have been included already in the overall sign of the self-energy diagram and are not part of our definition of the self-energy  $\Sigma$ .

renormalization constants. The (inverse) dressed quark propagator has been discussed above, its bare counterpart is given by

$$[S_0(k)]^{-1} = i\gamma \cdot k + Z_m m, \quad (50)$$

and contains the renormalized quark mass  $m$  from the Lagrangian of QCD. Since we work in the chiral limit,  $m = 0$ .

For this proof of concept we use a simple rainbow-ladder type approach where the dressed quark-gluon vertex  $\Gamma_\nu(k, q; l)$  is replaced by its bare counterpart, i.e.,

$$\Gamma_\nu(k, q; l) = Z_{1F}\gamma_\nu. \quad (51)$$

In Landau gauge, the gluon propagator is then given by

$$D_{\mu\nu}(l) = P_{\mu\nu}^T(l)D_T(l) + P_{\mu\nu}^L(l)D_L(l), \quad (52)$$

with momentum  $l = (\vec{l}, \omega_l)$ . The bosonic Matsubara frequencies are  $\omega_l = \pi T 2n_l$ . The projectors  $P_{\mu\nu}^{T,L}$  are transverse ( $T$ ) and longitudinal ( $L$ ) with respect to the heat bath vector aligned in four-direction and given by

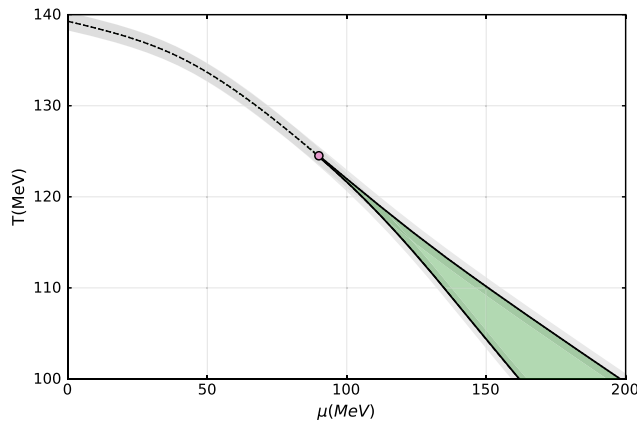
$$P_{\mu\nu}^T = (1 - \delta_{\mu 4})(1 - \delta_{\nu 4}) \left( \delta_{\mu\nu} - \frac{P_\mu P_\nu}{\vec{p}^2} \right),$$

$$P_{\mu\nu}^L = P_{\mu\nu} - P_{\mu\nu}^T, \quad (53)$$

where  $P_{\mu\nu} = \delta_{\mu\nu} - p_\mu p_\nu / p^2$  is the covariant transverse projector.

In our simple truncation scheme we replace the gluon propagator functions by the temperature and chemical potential independent effective running coupling

$$D_T(l) = D_L(l) = \frac{(Z_2)^2}{g^2(Z_{1F})^2} \frac{8\pi^2}{\omega^4} D e^{-l^2/\omega^2} \equiv D(l) \quad (54)$$



with parameters  $D = 1 \text{ GeV}^2$  and  $\omega = 0.6 \text{ GeV}$  [61] and specific powers of renormalization factors to preserve multiplicative renormalisability of the DSE. Essentially, the effective running coupling can be viewed as a convolution of the nonperturbative dressing of the gluon and the dressing for the leading  $\gamma_\mu$  structure of the quark-gluon vertex neglecting all medium effects. As reviewed in [62], this simple class of toy-models already displays the essential structure of the QCD phase diagram without, however, any claims of quantitative accuracy [63].

The order parameter for the chiral transition with temperature and chemical potential is the chiral condensate given by

$$\langle \bar{\psi}\psi \rangle = -Z_2 Z_m N_c T \sum_n \int \frac{d^3 k}{(2\pi)^3} \text{Tr}_D [S(k)], \quad (55)$$

where the trace is taken in Dirac space. Equivalently, also the value of the scalar quark dressing function  $B(\vec{k} = 0, n_k = 0)$  at lowest Matsubara frequency and vanishing three momentum may be used. The resulting phase diagram in this model is displayed in the left diagram of Fig. 2. One finds the second order chiral transition for small quark chemical potential  $\mu$ , a critical end-point and a first order transition at large  $\mu$ . At a fixed temperature slice below the critical one at  $\mu = 0$  we generically find two solutions for the DSEs for small chemical potential up to the transition line. The right hand diagram of Fig. 2 shows our order parameter for chiral symmetry for both solutions in the region with second order transition.

## B. Stability analysis

We now perform the calculation of  $\Gamma^{(2)}[\delta S]$  on fixed temperature slices using

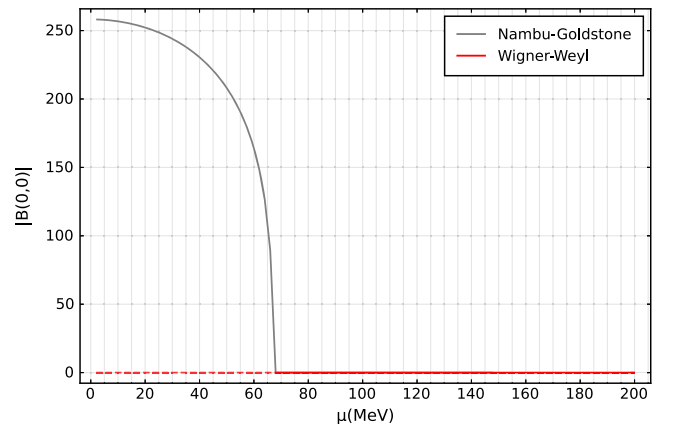


FIG. 2. Left diagram: phase diagram for the simple model described in the main text, systematic error of  $\pm 1$  MeV shown as the gray ribbon. Right diagram: Order parameters for the two solutions at fixed temperature slice  $T = 130$  MeV. The broken, and always stable, Nambu-Goldstone solution and the chiral Wigner-Weyl solution.

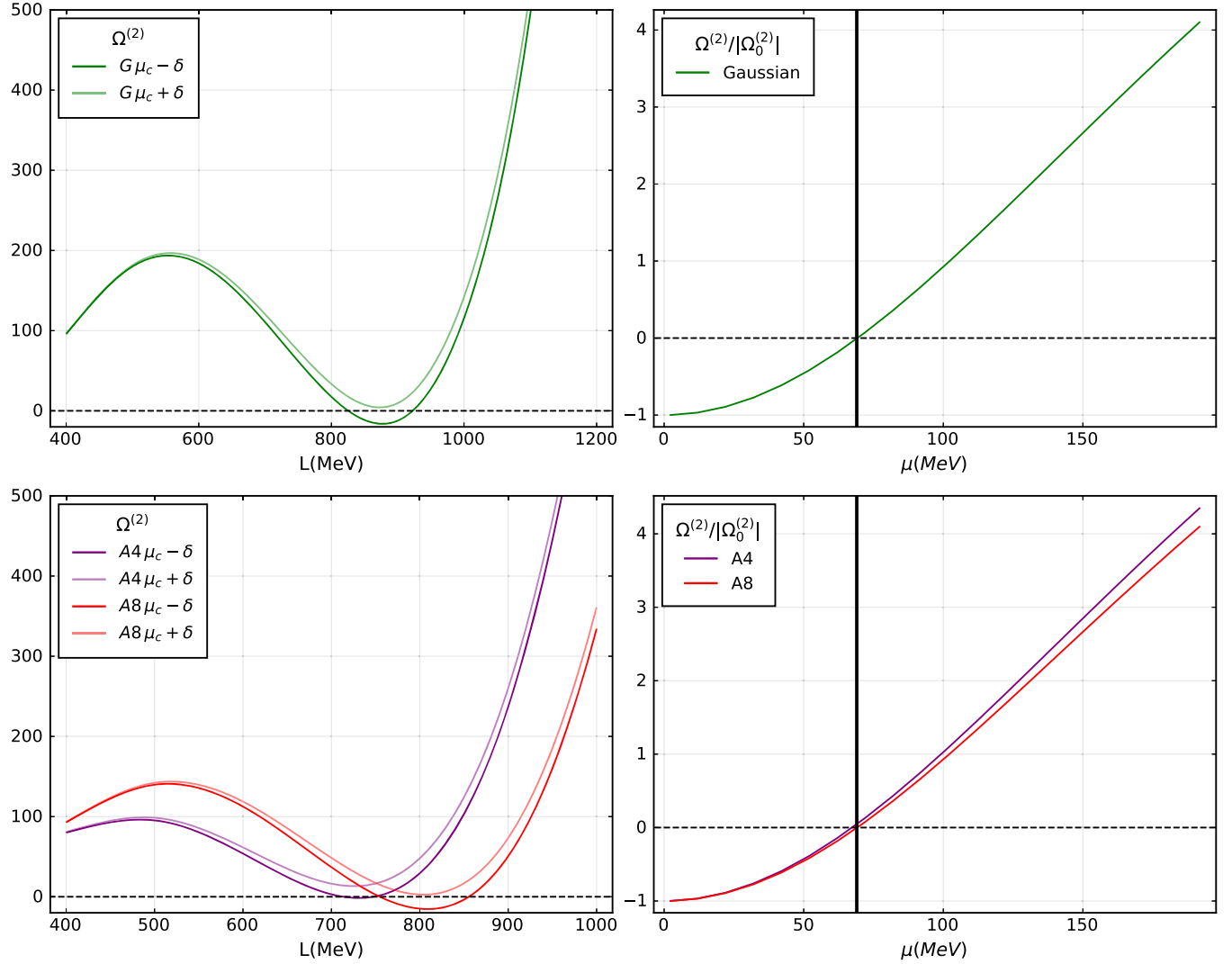


FIG. 3. Stability analysis for the homogeneous chiral phase transition test. Left diagrams: thermodynamic potential at a fixed value for temperature  $T = 130 \text{ MeV} < T_c(\mu = 0)$  and chemical potential  $\mu = \mu_c(T) \pm \delta = 69 \text{ MeV} \pm 1 \text{ MeV}$  as a function of the scale parameter  $L$ . For the upper diagram we used the Gaussian test-function for  $\delta m(k)$  and for the lower diagram the algebraic one, with  $N = 4$  (A4) and with  $N = 8$  (A8), see main text for further explanations. Right diagrams: normalized thermodynamic potential as a function of chemical potential on the same fixed temperature slice  $T < T_c(\mu = 0)$ . Note that, although the minimal  $L$  value changes with chemical potential, the figures on the right-hand side (rhs) were calculated with a fixed  $L$ , namely, the minimum  $L$  close to the critical chemical potential.

$$\delta S(k) = \frac{\delta m(k)}{\vec{k}^2 A(k)^2 + (k_4 + i\mu)^2 C(k)^2} \doteq \frac{\delta m(k)}{d(k)} \quad (56)$$

with denominator  $d(k) = \vec{k}^2 A(k)^2 + (k_4 + i\mu)^2 C(k)^2$  for several different test-functions for the mass which will be discussed shortly. The final expression for  $\Gamma^{(2)}$  is very simple

$$\Gamma^{(2)}[\delta m] = V_4 \int_k \left( -4N_c \frac{\delta m(k)^2}{d(k)} + 12N_c C_F Z_2^2 \int_q \frac{\delta m(k) \delta m(k-q)}{d(k) d(k-q)} D(q) \right). \quad (57)$$

We calculate the thermodynamic potential contribution, Eq. (17) and, since the relevancy is only on the sign (negative meaning unstable, positive meaning stable), we normalize it for better visualization:

$$\text{stability criterium : sign of } \frac{\Omega_\mu^{(2)}}{|\Omega_{\mu=0}^{(2)}|} = - \frac{\Gamma_\mu^{(2)}}{|\Gamma_{\mu=0}^{(2)}|}. \quad (58)$$

What remains to be specified is the mass function  $\delta m(k)$ . While in a general instability analysis the specific form of the energetically favored state is not known, here in our specific example the situation is different. From our explicit solutions of the quark-DSE in the chirally broken phase we

know that the resulting mass function is roughly given by a Gaussian. This is a direct consequence of our choice of the effective running coupling, Eq. (54). For the sake of our proof of concept, however, we will pretend to not know the specific shape, but test two different *Ansätze* for  $\delta m(k)$ . One is the expected Gaussian, the other a polynomial. Both *Ansätze* contain a free parameter,  $L$ , which correspond to an intrinsic scale. The functions are given by [64]

- (i) Gaussian  $\delta m(k) = \lambda \exp\left(-\frac{k_4^2 + \vec{k}^2}{L^2}\right)$
- (ii) Algebraic decaying  $\delta m(k) = \lambda \left(1 + \frac{k_4^2 + \vec{k}^2}{NL^2}\right)^{-N}$

This choice allows us to test, if we could infer the actual shape and scale of the energetically favored instability from the stability analysis alone.

Indeed, we find instabilities only for a range of values of the scale  $L$ . A typical situation is displayed in the upper left plot of Fig. 3, where we plot the instability condition for the Gaussian test-functions a function of the scale  $L$  for chemical potentials just before and just after the phase transition, respectively at  $\mu = 68$  MeV and  $\mu = 70$  MeV. Clearly, there is a region around the maximally unstable value  $L = 880$  MeV which is negative and therefore signals our chiral instability, but only for  $\mu < \mu_c$ . For smaller values of chemical potential, this negative region becomes larger, but never encompasses all possible scales  $L$ . For any chemical potential  $\mu > \mu_c$  the stability condition is positive for all scales  $L$ , signalling that the chirally symmetric phase is stable in this region. Plotting the stability condition for  $L = 880$  MeV on the upper right diagram of Fig. 3 as a function of chemical potential we can clearly identify the phase boundary at  $\mu = \mu_c$ .

Also for the algebraic *Ansätze* with power  $N = 4, \dots, 8$  we are able to identify an ( $N$ -dependent) optimal scale  $L$  (the minima approaches 880 MeV for larger  $N$ ) from the lower left diagram of Fig. 3 at the same chemical potentials. Observe that the minima become lower and lower for  $N \rightarrow \infty$ . The corresponding stability condition as a function of chemical potential, displayed in the lower right diagram of Fig. 3 shows that negative minima do occur for all powers of  $N > 3$  at smaller chemical potential and with increasing power  $N$  converge to the one of the Gaussian test-function in the diagram above. Thus, if we would not have considered the Gaussian test-function in the first place, this asymptotic behavior would have given us a clue as to try a Gaussian next. Therefore even in the absence of concrete knowledge of the shape of the stable solution of the propagator, we are able to extract corresponding information from a series of instability analyses using different *Ansätze*. In the case at hand, this would lead us to the correct Gaussian shape of  $\delta m(k)$  (recall again that the mass function of the chirally broken solution of the DSE is Gaussian in this truncation).

Finally, taking the Gaussian test-function, and performing the stability analysis within the full phase diagram of Fig. 2, we obtain the result shown in Fig. 4. The red region depicts where we find  $\Omega^{(2)}$  to be negative. Note that the

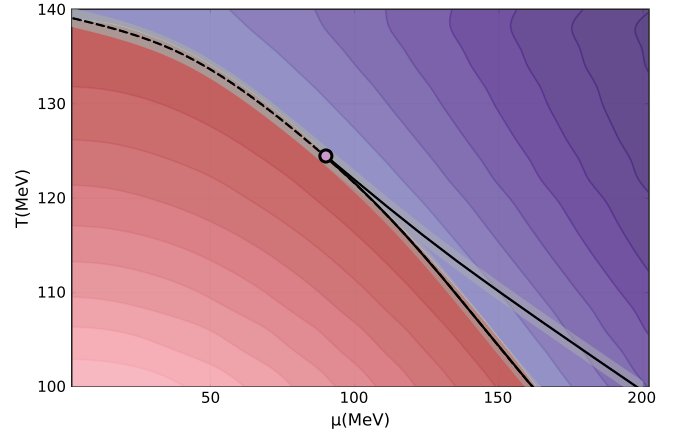


FIG. 4. Instability analysis of the chiral Wigner-Weyl solution. Red values indicate negativity (unstable), whereas purple indicates positivity (stable). The colour-gradient scale corresponds to  $\Omega^{(2)}$  in code units. Although only the sign of  $\Omega^{(2)}$  is relevant for the analysis, naturally small numbers correspond to a shallow stability well.

method is not only able to detect the second-order chiral transition line but also the left-hand spinodal of the first-order transition. This Wigner-Weyl spinodal line is notoriously difficult to accurately pinpoint numerically, since the calculation of  $\Omega^{(2)}(\Gamma^{(2)})$  itself can also be somewhat numerically intricate. The two terms in Eq. (57) are equally large in absolute value, but carry different signs [65]. Therefore, numerically, Eq. (57) corresponds to a subtraction of two big numbers resulting in something several orders of magnitude smaller, which is numerically delicate. Nevertheless, despite these technical difficulties, the method does not seem to ever *overestimate* the unstable region. This is extremely advantageous and increases confidence that whatever instabilities are found, they correspond to true instabilities and not inaccuracies of the numerical methods implemented.

## VII. CONCLUSIONS

In this work, we have proposed a novel framework for a stability analysis based on the nPI effective action of a given quantum field theory. We identified the well-known NJL stability analysis as the 1PI case of this more general framework. Within our approach, we intensively discussed a 2PI-based stability analysis that is suitable for QCD and beyond mean field NJL and QM models.

Although the QCD case is more complex than the one for models, it is possible to arrive at meaningful results. We performed a first cross-check of our approach for the case of the homogeneous chiral phase transition, where also explicit numerical results for both, the chirally broken and the chirally symmetric phase are present. We showed that our approach correctly identifies those areas of the phase diagram, where the chiral solution is unstable toward the



broken one. We also showed that different test functions lead to a similar result. Concerning future searches for instabilities of the homogeneous phase, this is a nice result. It shows we do not lose much of the generality of the shape-independent stability analysis. The test-function is not an *Ansatz* for the shape of the preferred phase, it is merely a tool.

One advantage of our analysis is that the truncation of the DSEs only concerns the description of the homogeneous phase. Therefore, the truncation only has to be good for the homogeneous case. This is a major improvement considering that inhomogeneous DSE calculations (such as in Müller *et al.* [34]) could be prohibitively hard with more sophisticated truncations.

The analysis as it stands is in principle ready to be applied to the search for inhomogeneous phases. One necessary first step for such an analysis, is the determination of the appropriate test-functions. As alluded to above, the form of Eq. (48) was already known *a priori*, which is not the case for inhomogeneous phases. Furthermore, the calculation of the 2PI effective action part  $\Gamma^{(2)}$  (or, equivalently, the thermodynamic potential  $\Omega^{(2)}$ ) is far more numerically intensive in this case. In addition, one must perform a search over  $\mu$  and  $T$  to find the phase transition lines, a task that was greatly alleviated in our cross-check by beforehand knowledge of the transition line. Moreover, optimization procedures of scales (like  $L$  in our case discussed above) in the test function have to be carried out at every analyzed point in the  $(T, \mu)$ -plane. This makes the search for inhomogeneous phases a viable but highly cost-intensive procedure that is relegated to future work.

### ACKNOWLEDGMENTS

We thank Wilhelm Kroschinsky, Ricardo Costa de Almeida and Jesuel Marques for immensely helpful discussions. This work has been supported by the Alexander von Humboldt Foundation, the Deutsche Forschungsgemeinschaft (DFG) through the Collaborative Research Center TransRegio CRC-TR 211 “Strong-interaction matter under extreme conditions” and the individual grant FI 970/16-1, the Helmholtz Graduate School for Hadron and Ion Research (HGS-HIRE) for FAIR and the GSI Helmholtzzentrum für Schwerionenforschung.

### APPENDIX A: FOURIER CONVENTIONS

Consider the quark propagator  $S(x, y)$  in Euclidean space at finite temperature, which in general is a function of two independent coordinates  $x, y \in V_4 = \mathbb{R}^3 \times [0, \frac{1}{T}]$ . Suppressing Dirac and other discrete indices we define the inverse propagator  $S^{-1}$  by

$$\int_z S^{-1}(x, z)S(z, y) = \delta(x, y), \quad (\text{A1})$$

where integrals in coordinate space are always understood to be over  $V_4$ .

The correct fermionic boundary conditions are implemented to these functions by relating them to their Fourier modes  $S(p, p')$  and  $S^{-1}(p, p')$ , respectively, as

$$S^{(-1)}(x, x') = \sum_{p, p'} e^{-i(p \cdot x - p' \cdot x')} S^{(-1)}(p, p') \quad (\text{A2})$$

with  $\sum$  as defined in Eq. (11). The corresponding inverse Fourier transforms are given by

$$S^{(-1)}(p, p') = \int_{x, x'} e^{i(p \cdot x - p' \cdot x')} S^{(-1)}(x, x'), \quad (\text{A3})$$

and one can easily check that the following relation holds:

$$\begin{aligned} \sum_k S^{-1}(p, k)S(k, p') &= \int_z e^{i(p-p') \cdot z} \\ &= (2\pi)^3 \delta(\vec{p} - \vec{p}') \frac{1}{T} \delta_{n, n'}, \end{aligned} \quad (\text{A4})$$

where  $n$  and  $n'$  label the Matsubara frequencies corresponding to  $p$  and  $p'$ , respectively.

In *homogeneous* matter the propagator only depends on the difference of the coordinates,  $S^{(-1)}(x, y) = \bar{S}^{(-1)}(x - y)$ . We then define

$$\bar{S}^{(-1)}(x - y) = \sum_p e^{-ip \cdot (x-y)} \bar{S}^{(-1)}(p), \quad (\text{A5})$$

which is consistent with Eq. (A1) for  $\bar{S}^{-1}(p)\bar{S}(p) = 1$ .

In general self-energies  $\Sigma = S^{-1} - S_0^{-1}$  are transformed in the same way as the inverse propagators. For *local* self-energies  $\Sigma(x, y) \equiv \Sigma(x)\delta(x, y)$  [see Eq. (28)] we obtain

$$\Sigma(p, p') = \int_x e^{i(p-p') \cdot x} \Sigma(x) \equiv \Sigma(p - p') \quad (\text{A6})$$

with the inverse transformation

$$\Sigma(x) = \sum_q e^{-iq \cdot x} \Sigma(q). \quad (\text{A7})$$

Considering space dependent but time-independent local self-energy fluctuations  $\delta\Sigma(x) \equiv \delta\Sigma(\vec{x})$  we then get

$$\delta\Sigma(q) = \int_{x_4} e^{iq_4 x_4} \int_{\vec{x}} e^{i\vec{q} \cdot \vec{x}} \delta\Sigma(\vec{x}) = \frac{1}{T} \delta_{q_4, 0} \delta\Sigma(\vec{q}) \quad (\text{A8})$$

with

$$\delta\Sigma(\vec{q}) = \int_{\vec{x}} e^{i\vec{q}\cdot\vec{x}} \delta\Sigma(\vec{x}). \quad (\text{A9})$$

## APPENDIX B: DERIVATIVES

Take a certain operator defined by a trace of some (continuous and dense) matrices in configuration or momentum space, say  $\Gamma = \text{Tr}[MN]$ , that is

$$\text{Tr}[MN] = \int_{x,y} M(x,y)N(y,x).$$

If we take a derivative, say

$$\frac{\delta\Gamma}{\delta M(x,y)}$$

that is

$$\begin{aligned} \frac{\delta\Gamma}{\delta M(x,y)} &= \int_{x',y'} \frac{\delta M(x',y')}{\delta M(x,y)} N(y',x') \\ &= \int_{x',y'} \delta(x-x')\delta(y-y')N(y',x') = N(y,x). \end{aligned}$$

By that, we note that the derivative of this trace yields not  $N(x,y)$  but  $N(y,x)$ . Therefore, when we write

$$\Gamma[S] = -\text{Tr} \log[S] - \text{Tr}[\mathbf{1} - S_0^{-1}S] + \Phi_{2\text{PI}}$$

$$\frac{\delta^n Z}{\delta J_{i_1} \cdots \delta J_{i_n}} = (-1)^n \frac{1}{Z[0]} \int \mathcal{D}\varphi \varphi_{i_1} \cdots \varphi_{i_n} e^{-(S[\varphi] - J_i \varphi_i - R_{ij}^{(2)} \varphi_i \varphi_j - R_{ijk}^{(3)} \varphi_i \varphi_j \varphi_k - \cdots)} \Big|_{J,R=0}. \quad (\text{C2})$$

However, one can also obtain higher-order  $n$ -point functions via differentiation with respect to the higher-order source terms. That is, for instance, the four-point function

$$\frac{\delta^4 Z}{\delta J_{i_1} \delta J_{i_2} \delta J_{i_3} \delta J_{i_4}} = \frac{\delta^2 Z}{\delta R_{i_1 i_2}^{(2)} \delta R_{i_3 i_4}^{(2)}} = -\frac{\delta Z}{\delta R_{i_1 i_2 i_3 i_4}^{(4)}} = \langle \varphi_{i_1} \varphi_{i_2} \varphi_{i_3} \varphi_{i_4} \rangle. \quad (\text{C3})$$

The connected generating functional is defined as

$$W[J, R^{(2)}, R^{(3)}, \dots] = \log Z[J, R^{(2)}, R^{(3)}, \dots] \quad (\text{C4})$$

the stationary point  $\delta\Gamma/\delta S(y,x) = 0$  is

$$\frac{\delta\Gamma}{\delta S(y,x)} = -S(x,y)^{-1} - S_0(x,y)^{-1} + \frac{\delta\Phi_{2\text{PI}}}{\delta S(y,x)} = 0 \quad (\text{B1})$$

and thus we identify the self-energy

$$\frac{\delta\Phi_{2\text{PI}}}{\delta S(y,x)} = \Sigma(x,y)$$

and the DSE

$$S(x,y)^{-1} = S_0(x,y)^{-1} - \Sigma(x,y). \quad (\text{B2})$$

## APPENDIX C: CONNECTED $n$ -POINT FUNCTIONS

Consider a theory with a classical action  $S[\varphi]$ . For simplicity we consider it as a function of a single field  $\varphi$ , however, the generalization is trivial. We can write its Euclidean-space generating functional, including  $n$  source terms for each  $n$ -point function, as simply

$$Z[J, R^{(2)}, R^{(3)}, \dots] = \int \mathcal{D}\varphi e^{-(S[\varphi] - J_i \varphi_i - R_{ij}^{(2)} \varphi_i \varphi_j - R_{ijk}^{(3)} \varphi_i \varphi_j \varphi_k - \cdots)}. \quad (\text{C1})$$

It is well known that the derivatives of such a functional with respect to the sources at the physical point are the  $n$ -point functions.

and differentiation of which will give rise to the connected  $n$ -point functions in the standard way [66,67], in particular for the 4-point function,

$$\begin{aligned} \frac{\delta^4 W}{\delta J_{i_1} \delta J_{i_2} \delta J_{i_3} \delta J_{i_4}} &= \frac{\delta^2 W}{\delta R_{i_1 i_2}^{(2)} \delta R_{i_3 i_4}^{(2)}} = -\frac{\delta W}{\delta R_{i_1 i_2 i_3 i_4}^{(4)}} \\ &= \langle \varphi_{i_1} \varphi_{i_2} \varphi_{i_3} \varphi_{i_4} \rangle_{\text{connected}}. \end{aligned} \quad (\text{C5})$$

From such, we may define its Legendre transform, the effective action

$$\Gamma[\phi, S_2, S_3, \dots].$$

- [1] A. W. Overhauser, Structure of nuclear matter, *Phys. Rev. Lett.* **4**, 415 (1960).
- [2] A. B. Migdal, Pi condensation in nuclear matter, *Phys. Rev. Lett.* **31**, 257 (1973).
- [3] A. B. Migdal, Pion fields in nuclear matter, *Rev. Mod. Phys.* **50**, 107 (1978).
- [4] F. Dautry and E. M. Nyman, Pion condensation and the sigma model in liquid neutron matter, *Nucl. Phys.* **A319**, 323 (1979).
- [5] M. Kutschera, W. Broniowski, and A. Kotlorz, Quark matter with neutral pion condensate, *Phys. Lett. B* **237**, 159 (1990).
- [6] W. Broniowski, Chiral waves in quark matter, *Acta Phys. Pol. B Proc. Suppl.* **5**, 631 (2012).
- [7] M. G. Alford, A. Schmitt, K. Rajagopal, and T. Schäfer, Color superconductivity in dense quark matter, *Rev. Mod. Phys.* **80**, 1455 (2008).
- [8] M. G. Alford, J. A. Bowers, and K. Rajagopal, Crystalline color superconductivity, *Phys. Rev. D* **63**, 074016 (2001).
- [9] J. A. Bowers, J. Kundu, K. Rajagopal, and E. Shuster, A diagrammatic approach to crystalline color superconductivity, *Phys. Rev. D* **64**, 014024 (2001).
- [10] A. K. Leibovich, K. Rajagopal, and E. Shuster, Opening the crystalline color superconductivity window, *Phys. Rev. D* **64**, 094005 (2001).
- [11] I. Giannakis, J. T. Liu, and H.-c. Ren, Angular momentum mixing in crystalline color superconductivity, *Phys. Rev. D* **66**, 031501 (2002).
- [12] M. Mannarelli, K. Rajagopal, and R. Sharma, Testing the Ginzburg-Landau approximation for three-flavor crystalline color superconductivity, *Phys. Rev. D* **73**, 114012 (2006).
- [13] G. Cao, L. He, and P. Zhuang, Solid-state calculation of crystalline color superconductivity, *Phys. Rev. D* **91**, 114021 (2015).
- [14] R. Anglani, R. Gatto, N. D. Ippolito, G. Nardulli, and M. Ruggieri, Superfluid and pseudo-Goldstone modes in three flavor crystalline color superconductivity, *Phys. Rev. D* **76**, 054007 (2007).
- [15] M. Sadzikowski, Coexistence of pion condensation and color superconductivity in two flavor quark matter, *Phys. Lett. B* **553**, 45 (2003).
- [16] M. Sadzikowski, Comparison of the nonuniform chiral and 2SC phases at finite temperatures and densities, *Phys. Lett. B* **642**, 238 (2006).
- [17] V. Schon and M. Thies, 2-D model field theories at finite temperature and density, *At Front. Part. Phys.* **8**, 1945 (2000).
- [18] M. Thies, From relativistic quantum fields to condensed matter and back again: Updating the Gross-Neveu phase diagram, *J. Phys. A* **39**, 12707 (2006).
- [19] G. Basar, G. V. Dunne, and M. Thies, Inhomogeneous condensates in the thermodynamics of the chiral NJL(2) model, *Phys. Rev. D* **79**, 105012 (2009).
- [20] R. Ciccone, L. D. Pietro, and M. Serone, Inhomogeneous phase of the chiral Gross-Neveu model, *Phys. Rev. Lett.* **129**, 071603 (2022).
- [21] D. Nickel, Inhomogeneous phases in the Nambu-Jona-Lasinio and quark-meson model, *Phys. Rev. D* **80**, 074025 (2009).
- [22] M. Buballa and S. Carignano, Inhomogeneous chiral condensates, *Prog. Part. Nucl. Phys.* **81**, 39 (2015).
- [23] M. Buballa, L. Kurth, M. Wagner, and M. Winstel, Regulator dependence of inhomogeneous phases in the (2 + 1)-dimensional Gross-Neveu model, *Phys. Rev. D* **103**, 034503 (2021).
- [24] L. Pannullo, M. Wagner, and M. Winstel, Inhomogeneous phases in the 3 + 1-dimensional Nambu-Jona-Lasinio model and their dependence on the regularization scheme, *Proc. Sci., LATTICE2022* (2023) 156.
- [25] L. Pannullo and M. Winstel, Absence of inhomogeneous chiral phases in 2+1-dimensional four-fermion and Yukawa models, *Phys. Rev. D* **108**, 036011, 2023.
- [26] W. Broniowski and M. Kutschera, Ambiguities in effective chiral models with cutoff, *Phys. Lett. B* **242**, 133 (1990).
- [27] T. L. Partyka and M. Sadzikowski, Phase diagram of the non-uniform chiral condensate in different regularization schemes at  $T = 0$ , *J. Phys. G* **36**, 025004 (2009).
- [28] D. V. Deryagin, D. Y. Grigoriev, and V. A. Rubakov, Standing wave ground state in high density, zero temperature QCD at large  $N(c)$ , *Int. J. Mod. Phys. A* **07**, 659 (1992).
- [29] E. Shuster and D. T. Son, On finite density QCD at large  $N(c)$ , *Nucl. Phys.* **B573**, 434 (2000).
- [30] Inhomogeneous chiral waves at large  $N_c$  have also been discussed in the context of quarkyonic matter [31].
- [31] T. Kojo, Y. Hidaka, L. McLerran, and R. D. Pisarski, Quarkyonic chiral spirals, *Nucl. Phys.* **A843**, 37 (2010).
- [32] W.-j. Fu, J. M. Pawłowski, and F. Rennecke, QCD phase structure at finite temperature and density, *Phys. Rev. D* **101**, 054032, 2020.
- [33] The authors identified a so-called moat regime where the wave-function renormalization constant in the scalar channel is negative. This is a necessary but not sufficient condition for instability of the homogeneous phase against small inhomogeneous fluctuations.
- [34] D. Müller, M. Buballa, and J. Wambach, Dyson-Schwinger study of chiral density waves in QCD, *Phys. Lett. B* **727**, 240 (2013).
- [35] M. Buballa and S. Carignano, Inhomogeneous chiral phases away from the chiral limit, *Phys. Lett. B* **791**, 361 (2019).
- [36] S. Carignano and M. Buballa, Inhomogeneous chiral condensates in three-flavor quark matter, *Phys. Rev. D* **101**, 014026 (2020).
- [37] A. Koenigstein, L. Pannullo, S. Rechenberger, M. J. Steil, and M. Winstel, Detecting inhomogeneous chiral condensation from the bosonic two-point function in the (1 + 1)-dimensional Gross-Neveu model in the mean-field approximation, *J. Phys. A* **55**, 375402, 2022.
- [38] M. Buballa, S. Carignano, and L. Kurth, Inhomogeneous phases in the quark-meson model with explicit chiral-symmetry breaking, *Eur. Phys. J. Special Topics* **229**, 3371 (2020).
- [39] P. Lakaschus, M. Buballa, and D. H. Rischke, Competition of inhomogeneous chiral phases and two-flavor color superconductivity in the NJL model, *Phys. Rev. D* **103**, 034030 (2021).
- [40] S. Carignano, M. Schramm, and M. Buballa, Influence of vector interactions on the favored shape of inhomogeneous chiral condensates, *Phys. Rev. D* **98**, 014033 (2018).
- [41] S. Carignano, M. Mannarelli, F. Anzuini, and O. Benhar, Crystalline phases by an improved gradient expansion technique, *Phys. Rev. D* **97**, 036009 (2018).

- [42] Strictly speaking, the thermodynamic potential is  $V\Omega_{\text{MF}}$  evaluated at this ground-state configuration, while the functional  $\Omega_{\text{MF}}[\phi_M]$  corresponds to an effective potential per volume. As customary, however, we call  $\Omega_{\text{MF}}[\phi_M]$  thermodynamic potential as well.
- [43] E. Nakano and T. Tatsumi, Chiral symmetry and density wave in quark matter, *Phys. Rev. D* **71**, 114006 (2005).
- [44] S. Carignano and M. Buballa, Two-dimensional chiral crystals in the NJL model, *Phys. Rev. D* **86**, 074018 (2012).
- [45] Remarkable exceptions are the 1 + 1 dimensional nonchiral and chiral Gross-Neveu models, where the inhomogeneous solutions have been constructed explicitly, namely the RKC and the CDW (chiral spiral), respectively [18].
- [46] Here we work with continuous Fourier transforms (see A) for convenience. On the other hand, typical inhomogeneities which have been discussed in this context are periodic in space, corresponding to a discrete reciprocal lattice (R.L.) in Fourier space. This is contained in our formalism as  $\delta\phi_M(\vec{q}) = \sum_{\vec{q}_n \in R.L.} \delta(\vec{q} - \vec{q}_n) \delta\phi_{M,\vec{q}_n}$  with discrete Fourier coefficients  $\delta\phi_{M,\vec{q}_n}$ . Using  $[\delta(\vec{q})]^2 = \delta(\vec{q})\delta(\vec{0}) = \delta(\vec{q}) \int d^3x = V\delta(\vec{q})$ , the squared Fourier transform in Eq. (9) should then be replaced by  $|\delta\phi_M(\vec{q})|^2 \rightarrow V \sum_{\vec{q}_n \in R.L.} \delta(\vec{q} - \vec{q}_n) |\delta\phi_{M,\vec{q}_n}|^2$ . The volume  $V$  then drops out and Eq. (9) becomes equal to the result presented in Ref. [35] and others.
- [47] This is indeed relevant as there is lively discussion about quantum fluctuations of Nambu-Goldstone bosons related to the symmetry breaking disordering the inhomogeneous system [48–50], e.g., into a quantum-pion-liquid (QPL) or a liquid-crystal (LC) [51–53], which further corroborates the importance of developing a method that goes beyond mean field within the scope of a stability analysis.
- [48] T.-G. Lee, E. Nakano, Y. Tsue, T. Tatsumi, and B. Friman, Landau-Peierls instability in a Fulde-Ferrell type inhomogeneous chiral condensed phase, *Phys. Rev. D* **92**, 034024 (2015).
- [49] Y. Hidaka, K. Kamikado, T. Kanazawa, and T. Noumi, Phonons, pions and quasi-long-range order in spatially modulated chiral condensates, *Phys. Rev. D* **92**, 034003 (2015).
- [50] R. Yoshiike, T.-G. Lee, and T. Tatsumi, Chiral pair fluctuations for the inhomogeneous chiral transition, *Phys. Rev. D* **95**, 074010 (2017).
- [51] R. D. Pisarski, A. M. Tselik, and S. Valgushev, How transverse thermal fluctuations disorder a condensate of chiral spirals into a quantum spin liquid, *Phys. Rev. D* **102**, 016015 (2020).
- [52] R. D. Pisarski and F. Rennecke, Signatures of moat regimes in heavy-ion collisions, *Phys. Rev. Lett.* **127**, 152302 (2021).
- [53] F. Rennecke and R. D. Pisarski, Moat regimes in QCD and their signatures in heavy-ion collisions, *Proc. Sci., CPOD2021* (2022) 016.
- [54] In order to avoid notation overload, we will use the round bracket notation  $\Gamma(T, \mu)$  to signify the functional  $\Gamma$  evaluated at the stationary point for fixed temperature and chemical potential, i.e.,  $\Gamma[S(T, \mu), T]|_{\text{Stationary}}$ . Note that  $\Gamma$  not only depends on  $T$  via the propagator  $S$  but also explicitly in the Matsubara sums.
- [55] J. Berges, N-particle irreducible effective action techniques for gauge theories, *Phys. Rev. D* **70**, 105010 (2004).
- [56] M. Carrington, Techniques for calculations with nPI effective actions, *EPJ Web Conf.* **95**, 04013 (2015).
- [57] J. M. Cornwall, R. Jackiw, and E. Tomboulis, Effective action for composite operators, *Phys. Rev. D* **10**, 2428 (1974).
- [58] This is trivially so, given that the first-order Taylor contribution comes with the first derivative of  $\Gamma$  with respect to  $S$  which is zero the stationary point by definition.
- [59] Since the calculation is based on a 1PI effective action the 2-point function is *not* defined self-consistently.
- [60] Dots denote dressed quantities; solid and wiggly lines represent quarks and gluons, respectively. All vertices are here bare.
- [61] R. Alkofer, P. Watson, and H. Weigel, Mesons in a poincare covariant Bethe-Salpeter approach, *Phys. Rev. D* **65**, 094026 (2002).
- [62] C. S. Fischer, QCD at finite temperature and chemical potential from Dyson-Schwinger equations, *Prog. Part. Nucl. Phys.* **105**, 1 (2019).
- [63] Often such an *Ansatz* is supplemented by an ultraviolet log-tail with a specific form dictated by perturbation theory. Here, we omit this log-tail for simplicity. We checked explicitly that all results remain qualitatively unchanged if the log-tail is included. Technically, including the log-tail and therefore establishing the correct perturbative ultraviolet behavior of QCD entails an additional complication:  $\Gamma[S]$  is highly divergent even in fully renormalized theories such as QCD and the then necessary subtraction has to be carried out with great numerical precision. This is possible but numerically demanding and we therefore resorted to the pure Gaussian for all calculations presented in this work deferring a more refined treatment to a future publication.
- [64] Here we fix the real/imag parts  $\lambda = (\lambda_1 + i\lambda_2)$  via Eq. (45) and force Eq. (44) by taking the complex conjugate of  $\delta m(k)$  for negative frequencies, i.e.,  $\delta m(-k_4, k) = \delta m(k_4, k)^*$ .
- [65] Due to this, note the importance of  $Z_2$  in Eq. (57). With this model for the gluon  $Z_2$  is indeed very close to 1, nevertheless, it drastically change the position of the critical line.
- [66] R. Rivers, *Path Integral Methods in Quantum Field Theory* (Cambridge University Press, Cambridge, England, 1988).
- [67] M. E. Peskin and D. V. Schroeder, *An Introduction to Quantum Field Theory* (Addison-Wesley, Reading, USA, 1995), ISBN 978-0-201-50397-5.